Prepared for submission to JINST

23rd International Workshop on Radiation Imaging Detectors
26-30 June, 2022
Riva del Garda, Italy

TCAD optimization of LGAD sensors for extremely high fluence applications

T. Croci,[a,1] A. Morozzi,[a] V. Sola,[e,d] P. Asenov,[b,a] A. Fondacci,[c] S. Giordanengo,[d] G. Borghi,[f] M. Centis Vignali,[f] G. Paternoster,[f] M. Boscardin,[f] M. Menichelli,[a] N. Cartiglia,[d] D. Passeri[c,a] and F. Moscatelli[b,a]

[a] *INFN, Perugia Unit, via A. Pascoli 23c, 06123 Perugia, Italy*
[b] *CNR-IOM, Perugia Unit, via A. Pascoli 23c, 06123 Perugia, Italy*
[c] *University of Perugia, Engineering Department, via G. Duranti 93, 06125 Perugia, Italy*
[d] *INFN, Torino Unit, via P. Giuria 1, 10125 Torino, Italy*
[e] *University of Torino, Physics Department, via P. Giuria 1, 10125 Torino, Italy*
[f] *FBK, via Sommarive 18, 38123 Trento, Italy*

E-mail: tommaso.croci@pg.infn.it

Abstract: The next generation of high-energy physics experiments at future hadronic colliders will require tracking detectors able to efficiently operate in extreme radiation environments, where expected fluences will exceed 1×10^{17} n_{eq}/cm^2. This new operating scenario imposes many efforts on the design of effective and radiation-resistant particle detectors. Low-Gain Avalanche Diode (LGAD) represents a remarkable advance because the radiation damage effects can be mitigated by exploiting its charge multiplication mechanism after heavy irradiation. To obtain the desired gain (about 10 – 20) on the sensor output signal, a careful implementation of the "multiplication" region is needed (i.e. the high-field junction implant). Moreover, a proper design of the peripheral region (namely, the guard-ring structure) is crucial to prevent premature breakdown and large leakage currents at very high fluences, when the bias voltage applied creates an electric field higher than 15 V/µm. In this contribution, the design of LGAD sensors for extreme fluence applications is discussed, addressing the critical technological aspects such as the choice of the active substrate thickness, the gain layer design and the optimization of the sensor periphery. The impact of several design strategies is evaluated with the aid of Technology-CAD (TCAD) simulations based on a recently proposed model for the numerical simulation of radiation damage effects on LGAD devices.

Keywords: Solid-state silicon detectors, Radiation-hard detectors, Tracking detectors, LGAD, TCAD simulation

[1]Corresponding author.

Contents

1 Introduction

The next generation of High Energy Physics (HEP) experiments, e.g. at the hadronic Future Circular Collider, will require tracking detectors able to efficiently operate in extreme radiation environments, where expected fluences will exceed $1 \times 10^{17}\ n_{eq}/cm^2$. This new operating scenario imposes many efforts on the design of particle detectors able to be radiation tolerant and to deliver time and position resolutions in the order of a few tens of picoseconds and a few tens of micrometers, respectively.

The Low-Gain Avalanche Diode (LGAD) technology represents a remarkable advance because the radiation damage effects can be mitigated by exploiting its charge multiplication mechanism [1] and it offers an intrinsic timing resolution of few tens of picoseconds [2]. To obtain a moderate internal gain (about $10 - 20$) and a stable operation, a careful implementation of the gain layer, i.e. the p^+ implant responsible for the signal multiplication , is needed. Moreover, a proper design of the peripheral region (namely, the guard-ring structure) is crucial to prevent premature breakdown and large leakage currents at high fluences.

In this contribution, the design and the optimization of LGAD sensors for extreme fluence applications are discussed, addressing the critical technological aspects such as the choice of the active substrate thickness, the design of the gain layer and the sensor periphery. The impact of several design strategies is evaluated with the aid of Technology-CAD (TCAD) simulations based on a recently proposed model for the numerical simulation of radiation damage effects on LGAD devices [3].

2 TCAD model for the numerical simulation of LGAD sensors

TCAD tools can be proficiently used to evaluate in advance the effects of layout and technological parameters on the device performance before its production. In this work, the analyses on existing structures and the new developments in the LGAD design have been done following detailed device-level simulations by means of the state-of-the-art Synopsys Sentaurus TCAD platform [4].

2.1 Layout and doping profile

The simulated device has been initially designed by neglecting the edges of the multiplication implant to focus the study on avalanche effect due to the high electric field generated by the gain layer. Moreover, the high sensitivity of the gain layer to its small technological variation has required a stringent mesh refinement and thus the need for a "quasi-1D approach", as depicted in figure 1.

The highly doped n-type strip and the moderately doped p-type gain layer have been modeled by means of a Gaussian analytical profile. Moreover, to take into account the acceptor-removal mechanism that occurs after the irradiation [5], the doping profile of the multiplication layer has been properly reduced for increasing values of fluence, by using the following analytical law:

$$N_A^{peak}(\Phi) = N_A^{peak}(0) \cdot e^{-c_A \cdot \Phi} \,. \tag{2.1}$$

According to that, the peak dose of the gain layer, N_A^{peak}, is recomputed as a function of the initial peak acceptor density, $N_A^{peak}(0)$, and the exponential dependence with the fluence, Φ, and the acceptor removal factor, c_A, which is calculated from the "Torino parameterization" [6].

2.2 Simulation outcomes and model validation

The steady-state behavior of the device has been simulated under different bias voltage and fluence conditions. The current-voltage curves of the irradiated devices have been obtained at 253 K and then scaled to 300 K to consider the temperature dependence of the current generated in the silicon bulk [7] and to have a direct comparison with experimental data [8]. Special attention has been devoted to the choice of the avalanche model, by investigating among the embedded available ones (e.g. Van Overstraeten-De Man [9], Okuto-Crowell [10] and University of Bologna [11]) as well as by extending the TCAD "portfolio" by adding different ones (e.g. Massey model [12]) through the code library customization [13]. Figure 2 top left shows significant differences between the models in terms of steady-state behavior. These are due to the different value of the impact ionization coefficients used in each model, and according to that, the Massey model presents the best agreement with the experimental data. In order to have a predictive insight into the electrical behavior and the charge collected by the LGADs up to the highest particle fluences expected in the future HEP experiments, the well validated "New University of Perugia" radiation damage model has been implemented within the TCAD simulation environment [14][15]. By coupling this numerical model, which allows to consider the comprehensive bulk and surface damage effects induced by radiation on silicon sensors, with the analytical law that describes the mechanism of acceptor removal in the gain layer, it has been possible to reproduce experimental data with high accuracy (see figure 2), demonstrating the reliability of the implemented simulation framework.

3 LGAD design and optimization

The good agreement obtained between simulation results and measurement data has allowed us to apply the newly developed model not only for the analysis of the device behavior, but also for the design and optimization of the future productions of LGAD sensors, considering their possible use in the next generation of collider experiments. To this purpose, in section 3.1 we compare different technology solutions in terms of substrate thickness and gain layer implant, and in section 3.2 the performances of different peripheral region designs are analyzed.

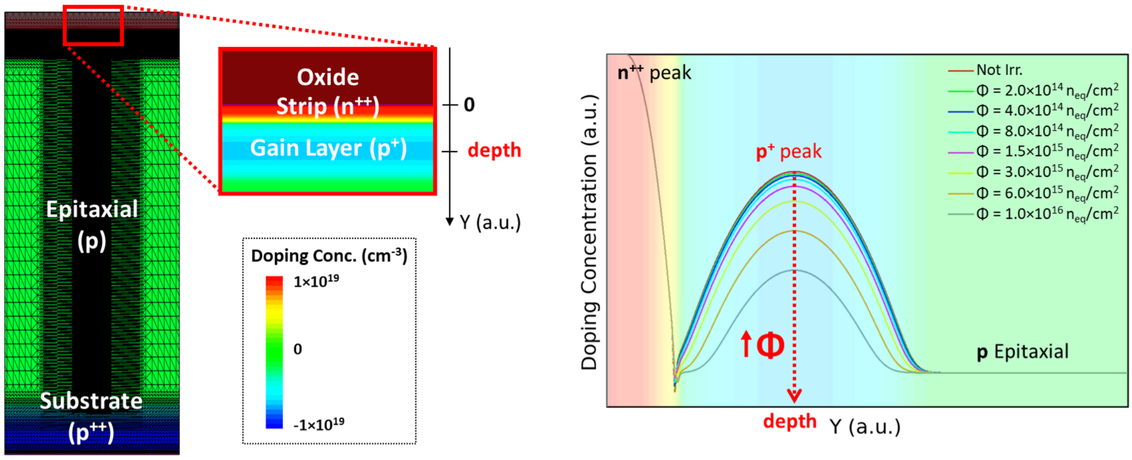

Figure 1. On the left, the layout of the LGAD device implemented within the TCAD environment. On the right, the simulated doping profiles. The n^{++}-strip and the p^{+}-gain implant are modeled by means of a Gaussian analytical profile. The gain layer doping profile is shaped according to the analytical law in eq. (2.1) to take into account the acceptor removal mechanism after the irradiation.

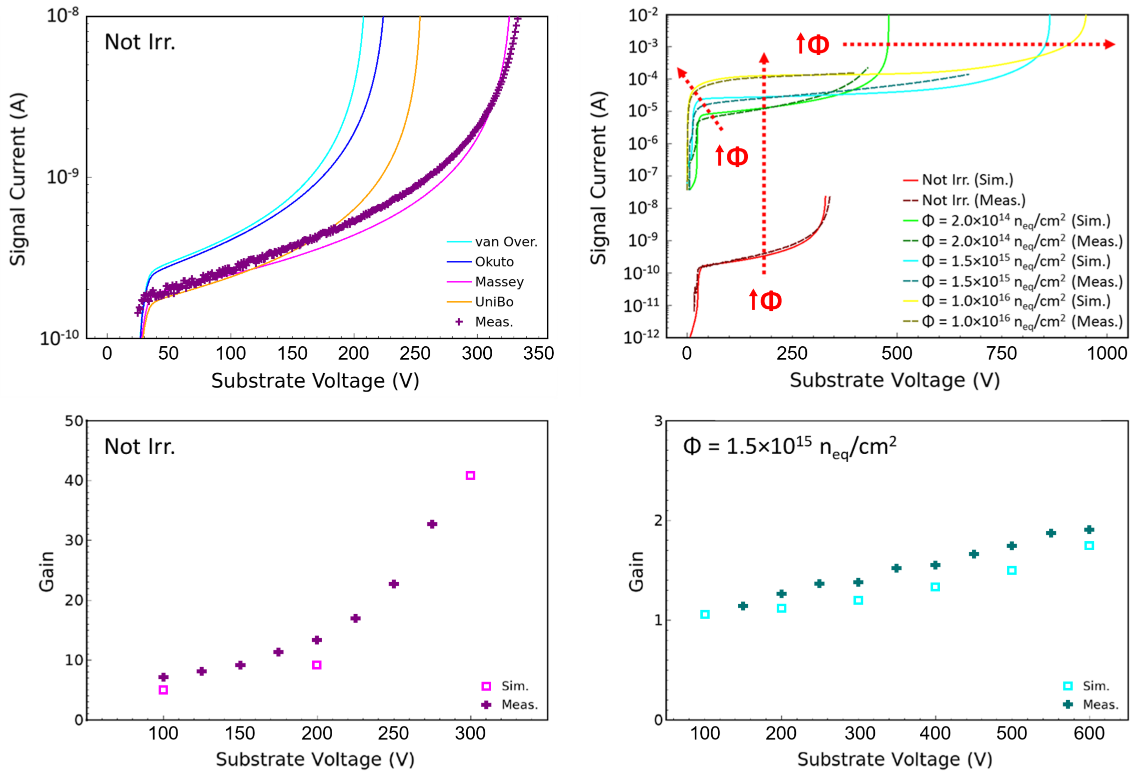

Figure 2. Comparison between simulated curves (Sim.) and experimental data (Meas.) carried out on a 55 μm-thick, 1 × 1 mm^2 LGAD device at 300 K [8]. Top left: current-voltage curves before irradiation for different avalanche models. Top right: current-voltage curves before and after irradiation. Bottom left: gain-voltage curves before irradiation. Bottom right: gain-voltage curves at the fluence of 1.5×10^{15} n_{eq}/cm^2.

3.1 The gain layer implant

Since the technological parameters of the gain layer implant strongly influence the multiplication capability of an LGAD device, different combinations of peak doping concentration, implantation depth and width have been investigated. In particular, three gain layer profiles have been designed and called "Shallow", "Standard" and "Deep" (see figure 3 left). For simplicity, these doping profiles are labeled with the letters A, B and C, and they are represented in red, green and blue, respectively. Figure 3 right reports the comparison between the simulated current-voltage curves for each considered gain layer doping profile for not irradiated devices. Differences in terms of depletion and breakdown voltage (V_{BD}) are clearly visible. For example, the "Deep" profile is characterized by a higher gain layer depletion voltage and a lower breakdown with respect to the other profiles, thus implying a smaller operating range of voltage. Moreover, a careful tuning of the peak dose of the gain layer implant has been done and a safety value of the breakdown voltage has been set at about 200 V to prevent the early breakdown of the device.

Once the peak dose of each gain layer profile has been fixed for not irradiated devices, the analysis focuses on the steady-state behavior and the gain evolution of the devices simulated at high irradiation fluences. Figure 4 left shows that the devices with different gain layer profiles behave like a PIN diode at the highest value of simulated fluence, i.e. $5 \times 10^{16}\ n_{eq}/cm^2$. The typical "knee" trend and the relatively high slope of the current-voltage curves before the breakdown are almost absent at that fluence. This implies that the LGAD device lost its multiplication power, despite the presence of active dopant, as confirmed by the unitary value of the gain-voltage curves in figure 4 right (see the cross markers): the remaining $N_A^{peak}(\Phi)$ does not allow for impact ionization to occur. Nevertheless, the simulations reveal that the signal multiplication capability is still preserved at a fluence of $1 \times 10^{16}\ n_{eq}/cm^2$. The gain-voltage curve of the "Shallow" profile (red square markers) shows that the value of the gain is roughly equal to ten when the sensor is biased at around 350 V and it is even equal to forty when the sensor is biased at the breakdown voltage ($V_{BD} \approx 380$ V). This is a hint of strong resilience of the "Shallow" profile to the radiation damage thanks to its higher residual acceptor density with respect to the other profiles.

Finally, sensors characterized by different substrate thicknesses have been simulated with the aim of investigating their electrical behavior once a specific gain layer doping profile design has been chosen (e.g. "Shallow"). The current-voltage curves of 15 µm, 30 µm and 45 µm-thick LGAD sensors are represented in figure 5 on the left, center and right, respectively. As mentioned before, by properly tuning the peak dose of the gain layer profile, it is possible to fix the breakdown voltage at a chosen value.

3.2 The sensor periphery

In figure 6, an example of a sensor periphery structure implemented within the TCAD environment is reported. The structure is composed by a collector ring, i.e. the bias-ring, a floating guard-ring (GR), and a scribe line. In particular, the floating GR has been specifically devised with both an n-deep and a p-stop implant. The latter helps to cut off the possible build-up of the so-called "inversion layer", i.e. a surface leakage current path between the collector ring and the n-deep implant itself, thus avoiding a direct connection between them [16].

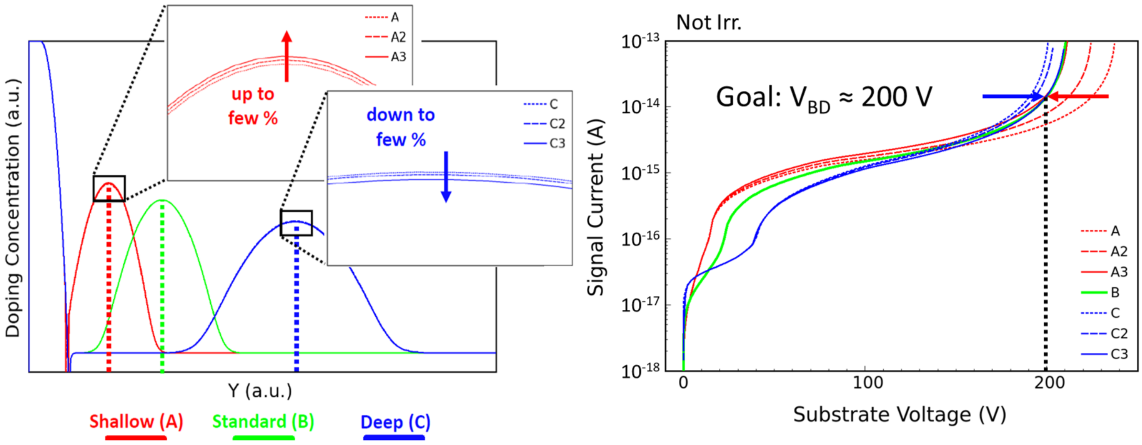

Figure 3. Gain layer sensitivity analysis. Impact of three different doping profiles (called "Shallow", "Standard" and "Deep" - on the left) on the simulated steady-state behavior of a 20 µm-thick LGAD device before irradiation at 300 K (see the current-voltage curves on the right). A variation of a few percentages of the gain layer peak dose is sufficient to produce a significant change of the breakdown voltage (V_{BD}).

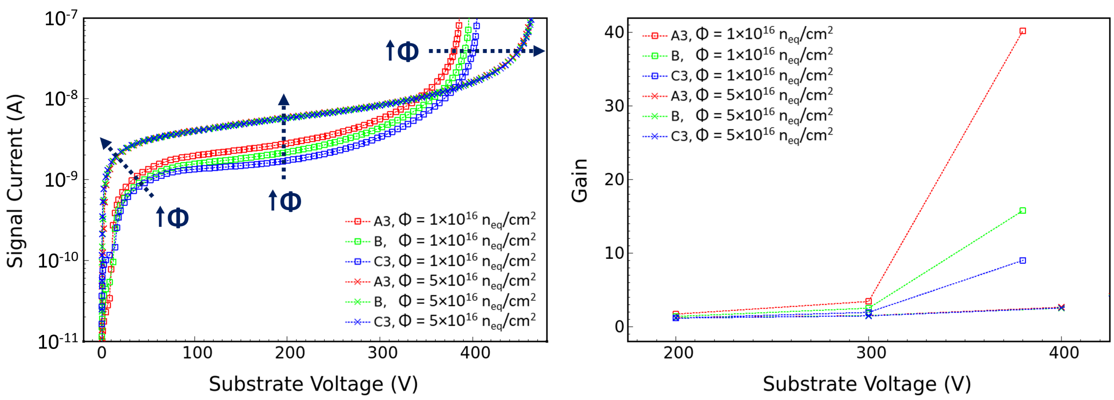

Figure 4. On the left, comparison between the steady-state behavior of the three gain layer profiles, and on the right, comparison between the corresponding gain-voltage curves simulated at the fluence of 1×10^{16} n_{eq}/cm^2 (square markers) and 5×10^{16} n_{eq}/cm^2 (cross markers).

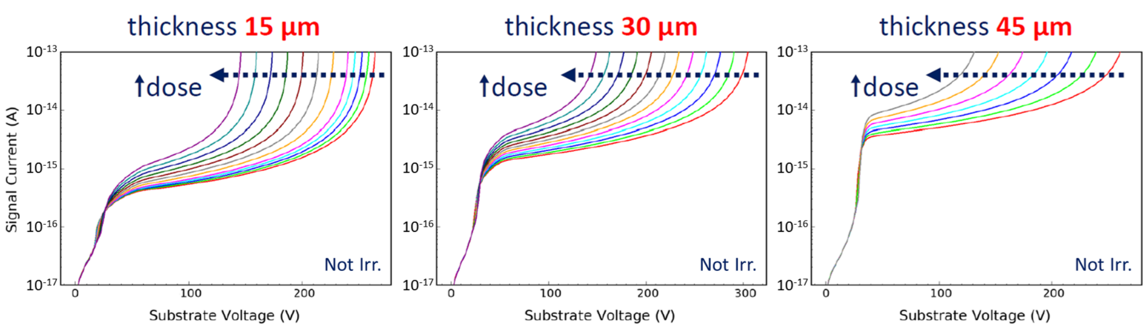

Figure 5. Steady-state behavior of a 15 µm (left), 30 µm (center), and 45 µm (right) thick LGAD sensor before irradiation at 300 K and tuning of the breakdown voltage by varying the peak dose of the gain layer ("Shallow" profile).

To allow the sensor to effectively operate in a harsh radiation environment, the optimization of the GR structure is a crucial task, specially when small substrate thicknesses are used. In figure 6 right, the V_{BD} trend as a function of a 15 µm, 25 µm, 35 µm and 45 µm-thick active substrate layer (A_L) before and after irradiation is shown. Not only the V_{BD} decreases by reducing A_L, as expected, but also the difference between the V_{BD} before and after irradiation decreases. The electrostatic potential and the electric field are represented in figure 7 left and right, respectively. They are both evaluated at a bias equivalent to V_{BD} and at a fluence of $1 \times 10^{15}\,\mathrm{n_{eq}/cm^2}$ as a function of the position along the surface region at a depth of 100 nm underneath the silicon-oxide interface. The sharp drop of the electrostatic potential in proximity of the implants implies high-electric-field peaks ($E_f \approx 40\,\mathrm{V/\mu m}$) which can trigger a premature breakdown. To ensure the stability and uniformity of the electric field distribution, several GR design strategies have been simulated (see table 1). As an example, as depicted in figure 8 left, a floating GR placed at a given distance from the collector ring allows to fix the voltage along the ring itself at an intermediate value, causing the redistribution of the electrostatic potential to a larger area and thus a significant reduction of the electric field, resulting in a higher V_{BD}. Moreover, by exploiting the concurrent action of bulk and surface damage to mitigate the creation of the inversion layer below the silicon-oxide interface [17], it is possible to design the periphery structure without p-stop isolation. As shown in figure 8 right, the V_{BD} is higher when the floating GRs do not have any p-stop implant, which might float to a potential value quite close to the bias, thus implying non-sustainable large voltage drops.

Table 1. Name and description of the simulated GR structures.

GR design	Description
full	1 or 3 floating GRs, with n-deep and p-stop
n-deep ONLY (X)	1 or 3 floating GRs, without p-stop implant (n-deep at X µm distance from the bias-ring)
p-stop ONLY (cont.)	1 or 3 floating GRs, without n-deep implant (with an electric contact over the p-stop)

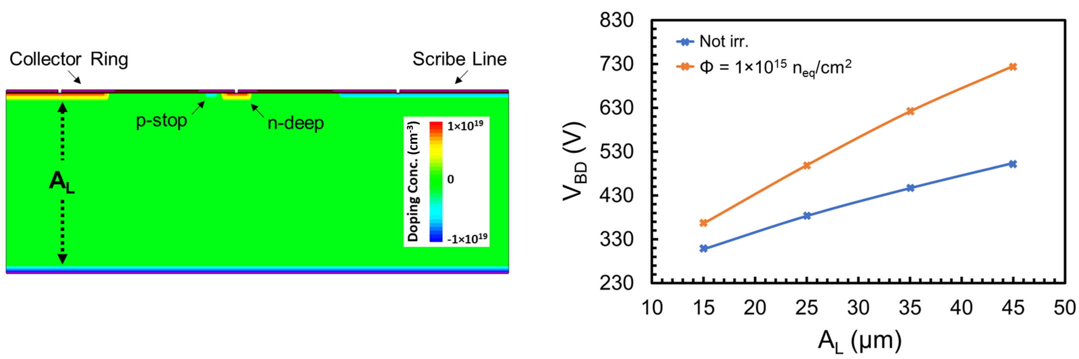

Figure 6. On the left: an example of a sensor periphery layout implemented within the TCAD environment. It consists of a collector ring, a floating guard-ring (i.e. the n-deep implant coupled with the p-stop one), and a scribe line. On the right: trend of the breakdown voltage, V_{DB}, as a function of the active substrate thickness, A_L, before and after irradiation ($\Phi = 1 \times 10^{15}\,\mathrm{n_{eq}/cm^2}$).

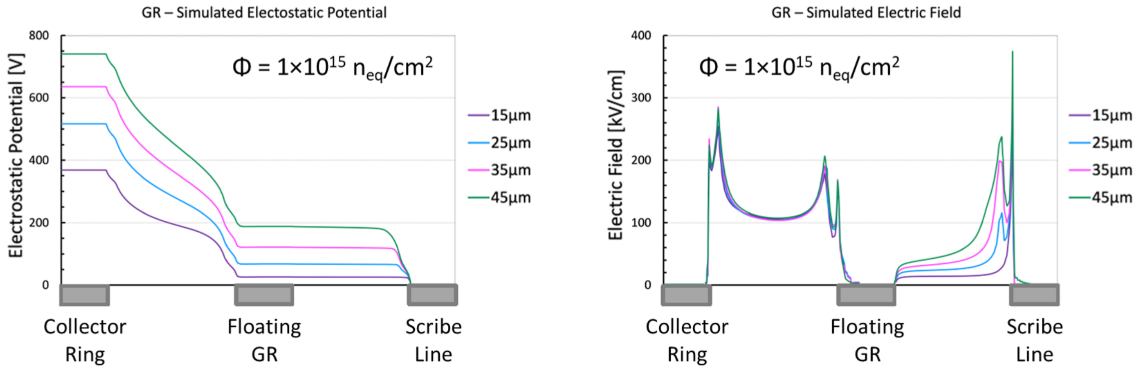

Figure 7. Simulated curves of electrostatic potential (on the left) and electric field (on the right), evaluated after the irradiation ($\Phi = 1 \times 10^{15}$ $\mathrm{n_{eq}/cm^2}$) at the breakdown voltage, expressed as a function of the position along the surface region of the sensor periphery, 100 nm underneath the silicon-oxide interface, for different values of the active substrate thickness (15 µm, 25 µm, 35 µm and 45 µm).

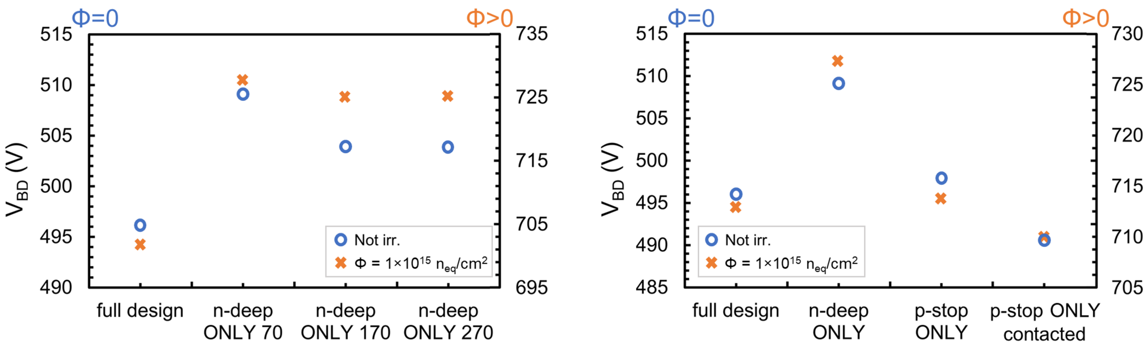

Figure 8. V_{BD} values obtained before and after irradiation ($\Phi = 1 \times 10^{15}$ $\mathrm{n_{eq}/cm^2}$) by simulating a 45 µm-thick, 500 µm-wide sensor periphery structure characterized by one floating GR (graph on the left) and three floating GRs (graph on the right), for different combinations of GR design strategies (see table 1).

4 Conclusions

In this work, the design and the optimization of LGAD sensors for extreme fluence applications, e.g. future collider experiments, have been presented. The impact of several design strategies has been evaluated with the aid of TCAD simulations based on a recently proposed model for the numerical simulation of radiation damage effects on LGAD sensors. Guidelines for a new production have been identified: *i)* a gain layer implant characterized by a highly-peaked and narrow high-field junction close to the n^{++}-strip electrode exhibits high residual acceptor density after a fluence of 1×10^{16} $\mathrm{n_{eq}/cm^2}$, i.e. high radiation tolerance; *ii)* different substrate thicknesses will be used, e.g. 15 µm, 20 µm, 35 µm and 45 µm, for which the impact of the technological parameters of the gain layer on the breakdown voltage has been evaluated in advance; *iii)* a sensor periphery with floating GR seems to be more effective without any p-stop implant, benefiting from the concurrent action of bulk and surface damage to mitigate the build-up of the inversion layer; *iv)* by properly positioning the floating GR(s) between the collector ring and the scribe line, it is possible to increase the V_{BD}, thus avoiding the occurrence of early breakdown.

Acknowledgments

This project has received funding from the European Union's Horizon 2020 research and innovation programme under GA No 101004761 and from the italian MIUR PRIN under GA No 2017L2XKTJ. The work is performed in collaboration with the INFN CSN5 "eXFlu" research project.

References

[1] G. Pellegrini et al., *Technology developments and first measurements of Low Gain Avalanche Detectors (LGAD) for high energy physics applications*, Nucl. Instrum. Meth. A **765** (2014) 12.

[2] N. Cartiglia et al., *Beam test results of a* 16 ps *timing system based on ultra-fast silicon detectors*, Nucl. Instrum. Meth. A **850** (2017) 83.

[3] T. Croci et al., *TCAD simulations of non-irradiated and irradiated Low-Gain Avalanche Diodes and comparison with measurements*, 2022 JINST **17** C01022.

[4] Synopsys Sentaurus TCAD (Online), available: https://synopsys.com/.

[5] M. Moll et al., *Acceptor removal - Displacement damage effects involving the shallow acceptor doping of p-type silicon devices*, October, 13-18, 2019 Lopud, Croatia. PoS (Vertex2019) 027.

[6] M. Ferrero et al., *An Introduction to Ultra-Fast Silicon Detectors*, 1st ed., CRC Press (2021).

[7] A. Chilingarov et al., *Temperature dependence of the current generated in Si bulk*, 2013 JINST **8** P10003.

[8] V. Sola et al., *First FBK production of* 50 µm *ultra-fast silicon detectors*, Nucl. Instrum. Meth. A **924** (2018) 360.

[9] R. Van Overstraeten and H. De Man, *Measurement of the ionization rates in diffused silicon p-n junctions*, Solid-State Electron. **13** (1970) 583.

[10] Y. Okuto and C. R. Crowell, *Threshold energy effect on avalanche breakdown voltage in semiconductor junctions*, Solid-State Electron. **18** (1975) 161.

[11] M. Valdinoci et al., "Impact-ionization in silicon at large operating temperature," 1999 International Conference on Simulation of Semiconductor Processes and Devices. SISPAD'99 (IEEE Cat. No.99TH8387), 1999, pp. 27-30, doi: 10.1109/SISPAD.1999.799251.

[12] D. J. Massey et al., *Temperature dependence of impact ionization in submicrometer silicon devices*, IEEE Trans. Electron Devices **53** (2006) 2328.

[13] M. Mandurrino et al., "Numerical Simulation of Charge Multiplication in Ultra-Fast Silicon Detectors (UFSD) and Comparison with Experimental Data," 2017 IEEE Nuclear Science Symposium and Medical Imaging Conference (NSS/MIC), 2017, pp. 1-4, doi: 10.1109/NSSMIC.2017.8532702.

[14] A. Morozzi et al., *TCAD advanced radiation damage modeling in silicon detectors*, October, 13-18, 2019 Lopud, Croatia. PoS (Vertex2019) 050.

[15] A. Morozzi et al., *TCAD modeling of surface radiation damage effects: a state-of-the-art review*, Front. Phys. **9** (2021) 617322.

[16] D. Flores et al., *Design and fabrication of an optimum peripheral region for low gain avalanche detectors*, Nucl. Instrum. Meth. A **821** (2016) 93.

[17] J.-O. Müller-Gosewisch et al., *Influence of surface damage and bulk defects on the interstrip isolation of p-type silicon strip sensors*, 2021 JINST **16** P07004.